J Mater Sci (2009) 44:4422–4428
DOI 10.1007/s10853-009-3670-x

Preparation and application of Cu/Cr hydrotalcite-like compounds

Qingze Jiao · Hongbo Liu · Yun Zhao · Zhe Zhang

Received: 9 March 2009 / Accepted: 6 June 2009 / Published online: 1 July 2009

Abstract A series of copper/chromium hydrotalcite-like compounds (Cu/Cr-HTlcs) with Cu/Cr molar ratios from 1:1 to 4:1 synthesized by coprecipitation reaction using NaOH and Na_2CO_3 as precipitation agents and their derived Cu/Cr mixed oxides (Cu/Cr-MO) were used in solid propellant for the first time. The structure, morphology and thermal behaviors were investigated using inductively coupled plasma optical emission spectrometry, X-ray diffraction, Fourier-transform infrared spectroscopy, N_2 volumetric measurements, transmission electron microscope, thermogravimetry, and differential thermal analysis. The results showed that a well crystallized Cu/Cr-HTlcs with ${CO_3}^{2-}$ as interlayer anions could be obtained with Cu and Cr molar ratio of 2:1, system pH value between 9 and 11, aging time longer than 24 h; the sample has a specific surface area of 107.8 $m^2\ g^{-1}$ and average pore diameter is 9 nm with pore volume of 0.34 $cm^3\ g^{-1}$; N_2 adsorption–desorption isotherm is type IVb with H_2-type hysteresis loop; thermal stability of the sample is relatively lower and the sample tends to be curled when the aging time is prolonged to 1 week at room temperature. Solid propellant with Cu/Cr-MO catalyst exhibit significantly higher burning rate of 9.64 $mm\ s^{-1}$ than those without catalyst (6.28 $mm\ s^{-1}$)/with $CuO \cdot Cr_2O_3$ catalyst (9.07 $mm\ s^{-1}$). Press index also decreases from 0.339 to 0.299, and mechanical performance on elongation for Cu/Cr-MO catalyzed propellant has a clear enhancement.

Q. Jiao (✉) · H. Liu · Y. Zhao · Z. Zhang
School of Chemical Engineering and Environment,
Beijing Institute of Technology, Beijing 100081,
People's Republic of China
e-mail: jiaoqz@bit.edu.cn

Abbreviations

Cu/Cr-HTlcs	Copper/chromium hydrotalcite-like compounds
Cu/Cr-MO	Cu/Cr mixed oxides
ICP-OES	Inductively coupled plasma optical emission spectrometry
XRD	X-ray diffraction
FT-IR	Fourier-transform infrared spectroscopy
TEM	Transmission electron microscope
TG	Thermogravimetry
DTA	Differential thermal analysis

Introduction

Hydrotalcite-like compounds (HTlcs) are bidimensional layered materials with the general formula $\left[M^{2+}_{(1-x)}M^{3+}_{x}(OH)_2\right]^{x+} \cdot A^{n-}_{x/n} \cdot mH_2O$. HTlcs consist of positively charged hydroxide sheets with intercalated anions (A^{n-}) and H_2O molecules [1]. The positive charge of the hydroxide sheets results from the isomorphous replacement of a fraction of the divalent cations (M^{2+}) by trivalent cations (M^{3+}). HTlcs can be varied with respect to composition, interlayer anions, and charge density. This diversity has led to many practical uses. Because of the many applications as adsorbents, catalysts and catalyst supports, HTlcs have received much attention in recent years [2]. All the bivalent metals from Mg^{2+} to Mn^{2+} form HTlcs, with the exception of Cu^{2+}, which forms HTlcs only when another bivalent cation is present [1]. It is well known that in octahedrally coordinated complexes the Cu^{2+} (d_9 configuration) exhibits a strong Jahn–Teller effect. While copper based HTlcs are good catalysts and catalysts precursors, they have been used as catalyst precursors for the catalytic removal of SO_x and NO_x [3, 4]. The catalytic production of hydrogen by steam reforming of methanol has been carried out over several Cu containing HTlcs [5]. Shiau et al. [6] indicate that Cu/Cr catalysts have a good activity for ethanol dehydrogenation, and Cu/Cr based catalyst is also effective for the dehydrogenation of isoamyl alcohol to isovaleraldehyde [7]. It is also known that HTlcs containing transition metals tend to exhibit enhanced catalytic activity owing to the presence of redox and Lewis sites that may be combined with the structural and geometric features to yield solids with the desired properties. In the past decade, preparations and applications of many HTlcs have been reported [8], but very little report is available on preparation of Cu/Cr-HTlcs without other bivalent cation. Thus it is quite necessary to prepare Cu/Cr-HTlcs via coprecipitation reaction.

Solid propellants are used for space, ballistic, tactical and assist propulsion, and solid composite propellants in use today are mixtures of prepolymer (binder), aluminum fuel and oxidizer salts like Ammonium perchlorate [9]. Combustion of solid propellants is a complex process of mass and heat transfer [10]. The burning rates mainly depend on specific surface areas between oxidant and fuel, and catalytic behavior of combustion catalysts. Burning rate catalysts are always of great interest in order to improve the ballistics of the rocket design, because of advantages such as significant increase in propellant burning rates, shorter ignition delays and shorter agglomerate burning times [11]. Recently it was found that the catalytic performance of nanoscale catalysts was superior to that of microscale ones [12, 13] for the reason that components of the catalysts can be mixed in nanoscale which leads to a strong “comparative effect”. CuO and Cr_2O_3 are considered as potential burning rate catalysts for composite solid propellants [14, 15]. Most studies of burning rate catalysts are prepared by room temperature solid-state reaction and homogeneous phase precipitation route, while there is no report available for Cu/Cr-mixed oxides (Cu/Cr-MO) obtained by hydrotalcite derived mixed oxides.

This study reports the synthesis and characterization of Cu/Cr-HTlcs without other bivalent cation by coprecipitation reaction. It is aimed at offering a precursor of copper and chromium mixed oxides with large surface area and high metal dispersion. To the best of our knowledge, this is the first report on using HTlcs derived mixed oxides as catalysts for combustion of solid rocket propellants.

Experimental

Preparation of Cu/Cr-HTlcs

Four samples of HTlcs with Cu/Cr molar ratios 1:1, 2:1, 3:1, and 4:1 (assigned as Cu_1Cr, Cu_2Cr, Cu_3Cr and Cu_4Cr, respectively) were prepared by coprecipitation reaction at high supersaturation. An aqueous solution (300 mL) containing appropriate amount of Cu $(NO_3)_2 \cdot 6H_2O$ and Cr $(NO_3)_3 \cdot 9H_2O$ with $[Cu^{2+}] = 0.06$ M was added dropwise with vigorous stirring into 300 mL of NaOH and Na_2CO_3 solutions ($[OH^-] = 1.8[Cu^{2+}] + 1.8[Cr^{3+}]$, $[CO_3^{2-}] = 2[Cr^{3+}]$). The addition took about 0.5 h. The pH is kept between 9 and 11, and the resulting suspension was maintained at 333 K for 24 h. The product was filtered, washed thoroughly with distilled water and dried overnight at 353 K in an oven.

Preparation of Cu/Cr-MO

The Cu/Cr-MO catalysts were obtained by calcination of Cu/Cr-HTlcs precursors, which were carried out in muffle furnace with temperature controller. The sample were heated at constant heating rate 5 K min^{-1} up to 773 and 1073 K (assigned as Cu/Cr-MO-773 and Cu/Cr-MO-1073), respectively, kept at this temperature for 3 h and then cooled in the oven down to ambient temperature.

For comparison, $Cu(OH)_2$ and $Cr(OH)_3$ were synthesized with the similar procedures to those for Cu/Cr hydrotalcite precursors in the absence of Cr $(NO_3)_3 \cdot 9H_2O$ and Cu $(NO_3)_2 \cdot 6H_2O$, respectively. CuO and Cr_2O_3 were prepared by calcination of the precursors at 773 K, and then $CuO \cdot Cr_2O_3$ catalysts (assigned as $CuO \cdot Cr_2O_3$-773) were obtained by mechanically mixing those CuO and Cr_2O_3 in appropriate ratios.

Characterization of Cu/Cr-HTlcs

Elemental chemical analysis for Cu and Cr were carried out by inductively coupled plasma optical emission spectrometry (ICP-OES), using a JY, model ULTIMA, after dissolution of the sample in 0.1 M HNO_3. Powder X-ray diffraction (XRD) patterns were recorded using PANalytical X'Pert PRO MPD diffractometer, using Cu K_α ($\lambda = 1.5406$ Å) radiation operating with 40 kV and 150 mA for phase identification and orientation. Scans were made in the 5°–75° 2θ region using a scan rate of 3° min^{-1}. The Fourier-transform infrared spectroscopy (FT-IR) spectra were recorded using the KBr pellet technique on a Brucker VECTOR22 spectrometer in 4000–450 cm^{-1} to identify functional groups present. A Quantachrome NOVA 1200e with Surface Area & Pore Size Analyzer was used to obtain the specific surface area and pore structure of the catalysts. Transmission electron microscope (TEM) was taken on a Hitach-800 electron microscope, operating at 100 KV to observe the morphology and measure the size of the particles. Thermogravimetry (TG) was carried on a Pyris-1 thermogravimetric analyzer (Perkin Elemer, USA) and differential thermal analysis (DTA) was carried on a HCT-2 thermobalance. Analysis was done from 323 to 873 K at a heating rate of 10 K min^{-1} under nitrogen (40 mL min^{-1}) for thermal stability analysis.

Catalytic performance on combustion of solid rocket propellant

Propellant samples were burned in a nitrogen-flushed window bomb in order to measure the steady burning rate, and pressure was kept constant during the whole combustion process with a feedback pressure control system. The burning rate was measured in the range 30–110 bar with the catalysts dosage of 0.5 wt%. The catalytic performances of different catalysts on combustion of solid rocket propellant were studied under 60 bar with the catalyst dosage of 1.0 wt%.

Results and discussion

Composition of Cu/Cr-HTlcs

The results of chemical analysis for samples with different Cu/Cr molar ratios are shown in Table 1. The Cu/Cr molar ratios from 1:1 to 4:1 observed for the precipitated solids are in good agreements with the nominal ratios used for preparing the starting solutions. The results show that the precipitation process is sufficient, and we can indicate that Cu/Cr-HTlcs samples with the molar ratio of Cu/Cr from 1:1 to 4:1 are successfully prepared by coprecipitation reaction.

Structure of Cu/Cr-HTlcs

The X-ray patterns of the synthesized samples at 333 K for 24 h with the molar ratio of Cu/Cr from 1:1 to 4:1, i.e. Cu_1Cr, Cu_2Cr, Cu_3Cr, and Cu_4Cr-HTlcs, are show in Fig. 1. In each case, the XRD patterns exhibit the characteristic reflections of HTlcs material. Lower diffraction intensity is observed for the Cu_1Cr-HTlcs sample than for others, perhaps it is an amorphous phase which represents the trend of the formation of Cu/Cr-HTlcs. While Cu_2Cr-HTlcs sample shows sharp and intense diffraction peaks. There is no separate phase for the Cu_1Cr and Cu_2Cr-HTlcs samples. XRD patterns for Cu_3Cr and Cu_4Cr-HTlcs samples show that they contain hydrotalcite as the main component, exhibiting sharp and symmetric reflections for the basal (003) and (006). Little CuO impurities also can be observed from XRD patterns, and the diffraction intensity of CuO phase become stronger with the increasing Cu/Cr molar ratio.

Table 1 ICP-OES analysis results for Cu/Cr-HTlcs with Cu/Cr molar ratios from 1:1 to 4:1

Sample		Cu_1Cr	Cu_2Cr	Cu_3Cr	Cu_4Cr
Cu/Cr	Int.	1:1	2:1	3:1	4:1
	Calc.	1.009:1	2.007:1	2.993:1	3.960:1

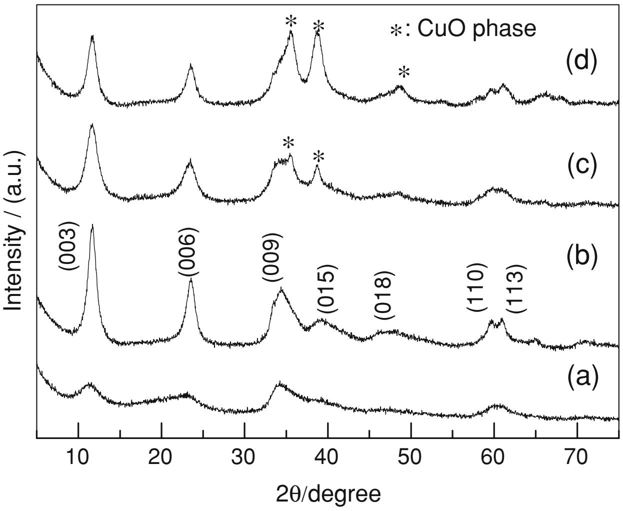

Fig. 1 XRD patterns for Cu/Cr-HTlcs with different Cu/Cr molar ratios for (a) 1:1; (b) 2:1; (c) 3:1; (d) 4:1

For Cu_1Cr and Cu_2Cr-HTlcs samples, no CuO phase was observed under our experimental conditions. This may be explained by the lower Cu^{2+} ions content which weakened the Jahn–Teller effect of Cu. With the increase of copper content, CuO phase can be observed (Fig. 1c), and the intensity of CuO phase became stronger (Fig. 1d), which ascribed to the higher content of Cu and the vigorous Jahn–Teller effect leading a difficulty for Cu^{2+} entering into sheets, and the redundant Cu^{2+} in the formation of $Cu(OH)_2$ and finally changed into CuO as reported by Cudennec and Lecerf [16]. In general, synthesis of single HTlcs phase containing Cu^{2+} as the only divalent metal is somewhat difficult. The lattice parameter c is three times the distance from the center of one layer to the next. The value of c ($= 3d_{003}$) is a function of the average charge of the metal cations, the nature of the interlayer anion and the water content. The effect of system pH value on d_{003} (the basal spacing calculated from the 003 reflection position in the XRD pattern) [1, 17] of Cu/Cr-HTlcs is shown in

Fig. 2. It can be observed that d_{003} increase rapidly with the increase of system pH values, and it reaches a value of 7.95 Å with the corresponding parameter *c* of 23.85 Å (a well crystallized Mg/Cr-HTlcs with CO_3^{2-} as interlayer anions has a *c* parameter value of 23.4 Å) [1] when pH is about 9.0. Then it remains at this constant value in spite of the continuous increasing system pH values, which represents that the Cu/Cr-HTlcs is efficiently precipitated and the growth of brucite-like layer is well finished. It can be indicated that the system pH values should be controlled above 9.0 in order to obtain a well crystallized Cu/Cr-HTlcs with CO_3^{2-}as interlayer anions.

IR analysis is not a diagnostic tool for HTlcs, but can be useful to identify the presence of foreign anions in the interlayer between the brucite-like sheets. The FT-IR spectrum of Cu_2Cr-HTlcs is shown in Fig. 3. The intense and broad band observed at about 3300–3500 cm^{-1} is assigned to O–H stretching ($\nu_{O\text{–}H}$) due to the presence of hydroxyl as well as both adsorbed and interlayer water. In the range of 1350–1500 cm^{-1}, the absorption bands of the anions are attributed to the ν_3 asymmetric stretching of CO_3^{2-}. And the sharp band observed at about 530 cm^{-1} can be attributed to the metal oxygen stretching. This is in good agreement with the X-ray results that confirmed a well crystallized Cu/Cr-HTlcs with CO_3^{2-} as interlayer anions was obtained.

The specific surface area measured for Cu_2Cr-HTlcs is 107.8 $m^2\ g^{-1}$ and the average pore diameter is 9 nm (as shown in Fig. 4) with pore volume of 0.34 $cm^3\ g^{-1}$. Figure 5 shows the N_2 adsorption–desorption isotherm graphic of Cu_2Cr-HTlcs. Based on the classification by Rouquerol et al. [18], the isotherm of the sample is type IVb. The plateau at high p/p_0 and the small N_2 adsorption at lower p/p_0 values are characteristics of IVb. The sample presents a H_2-type hysteresis loop according to the

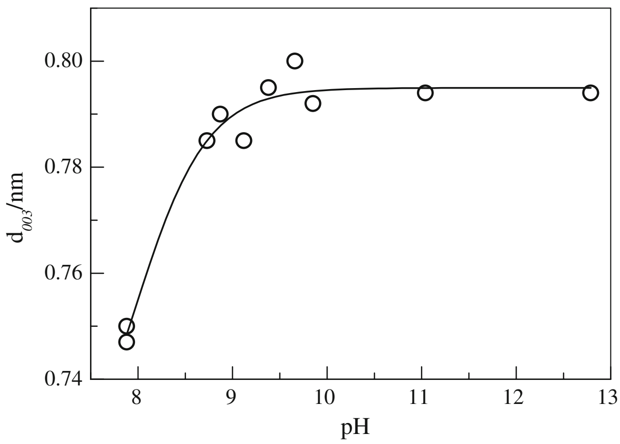

Fig. 2 Effect of system pH value on d_{003} for Cu/Cr-HTlcs with molar ratio of 2:1 aging for 24 h

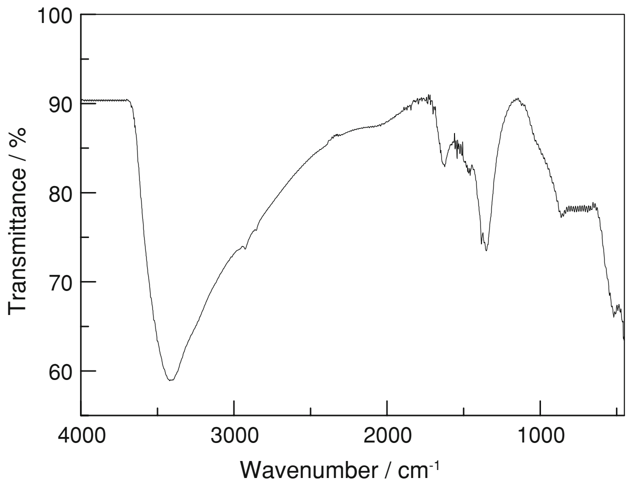

Fig. 3 FT-IR spectra for Cu/Cr-HTlcs with molar ratio of 2:1 aging for 24 h

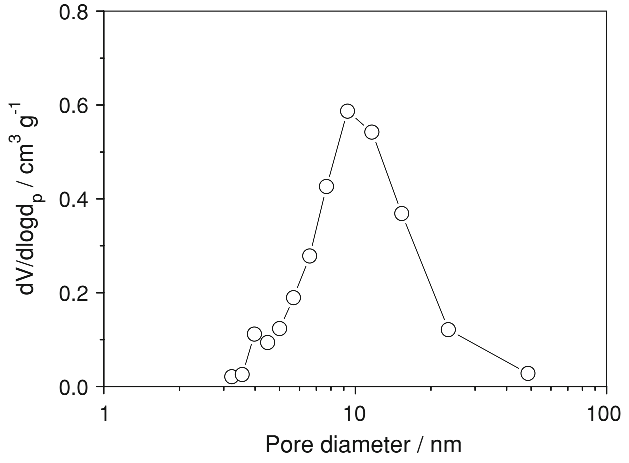

Fig. 4 Pore diameter distribution for Cu/Cr-HTlcs with molar ratio of 2:1 aging for 24 h

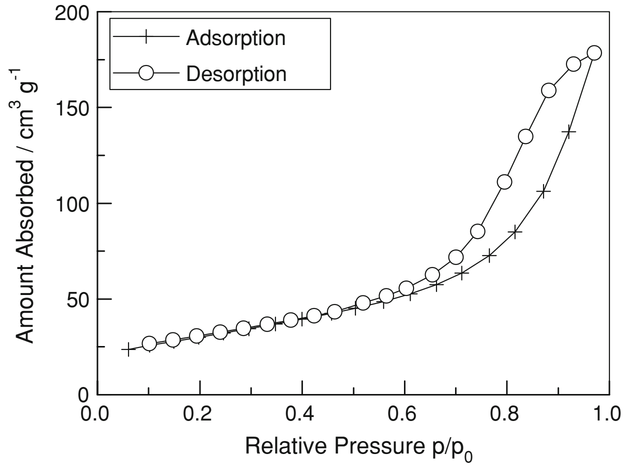

Fig. 5 N_2 Adsorption–desorption isotherm at 77 K for Cu/Cr-HTlcs with molar ratio of 2:1 aging for 24 h

classification of IUPCA, which represents a typical of materials with slit-shaped pores or aggregates of platelet-like particles. The specific surface area and pore size makes it attractive for catalytic application.

Morphology of Cu/Cr-HTlcs

All the samples prepared with different Cu/Cr molar ratios aged at 353 K for 24 h show homogenous hexagons, thus the morphology of Cu_2Cr-HTlcs with different aging time was investigated. Figure 6 shows the TEM images of Cu_2Cr-HTlcs samples with different aging time. The micrograph of the sample (a) shows irregular flakes; sample (b) shows homogenous hexagons with average crystallite size in the range of 30–50 nm. When aging time is prolonged to 1 week, sample (c) shows a mixture of hexagons and curl flakes; while when aging time reaches 1 month, almost all of the sample (as shown in graph (d)) exhibit curled flakes. It could be explained by the dynamics of crystal growth that the particles tend to grow in the energy minimized direction, thus the outspread hexagons begin to curl and finally changes into curled flakes. And on the other hand, the Jahn–Teller effect of Cu results in a distortion of texture, which leads to instability of the sample and this instability indirectly makes the hexagons in favor of changing to curled flakes. This may contribute to potential performance for catalytic applications.

Thermal stability of Cu/Cr-HTlcs

To understand the decomposition procedure of the Cu/Cr-HTlcs, the TG, DTG and DTA profiles of Cu_2Cr-HTlcs sample are analyzed in detail. As shown in Figs. 7 and 8, three weight loss stages can be observed on TG curve, corresponding to the three endothermic peaks around 440, 530, and 740 K on DTA profile, demonstrating that the decomposition proceeded in three steps. The first step is identified by a DTG minimum at 370–440 K corresponds to removal of weak bonded water molecular and the water absorbed on the sample surface. This step is immediately followed by a second one, up to ca. 530 K, this usually attributes to the loss of interlayer water and some hydroxyl groups of the brucite-like layer. The DTG curve also exhibits a wide peak ca. 440–530 K. The last step is up to 740 K and the structure of hydrotalcite collapses with the loss of hydroxyl groups of the brucite-like layer, as well as the carbonate and interlayer anions. A clear peak around

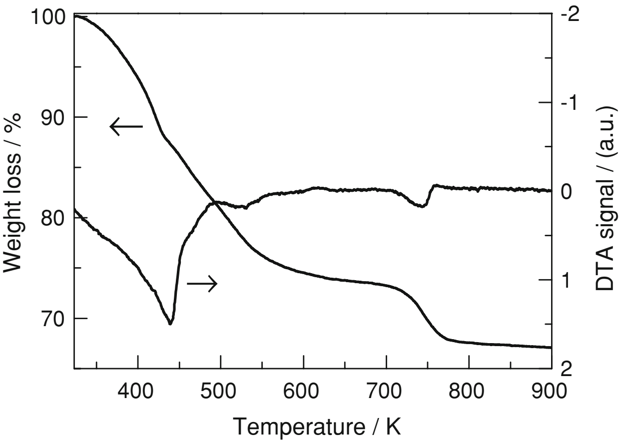

Fig. 7 TG and DTA curves for Cu/Cr-HTlcs with Cu/Cr molar ratios of 2:1 aging for 24 h

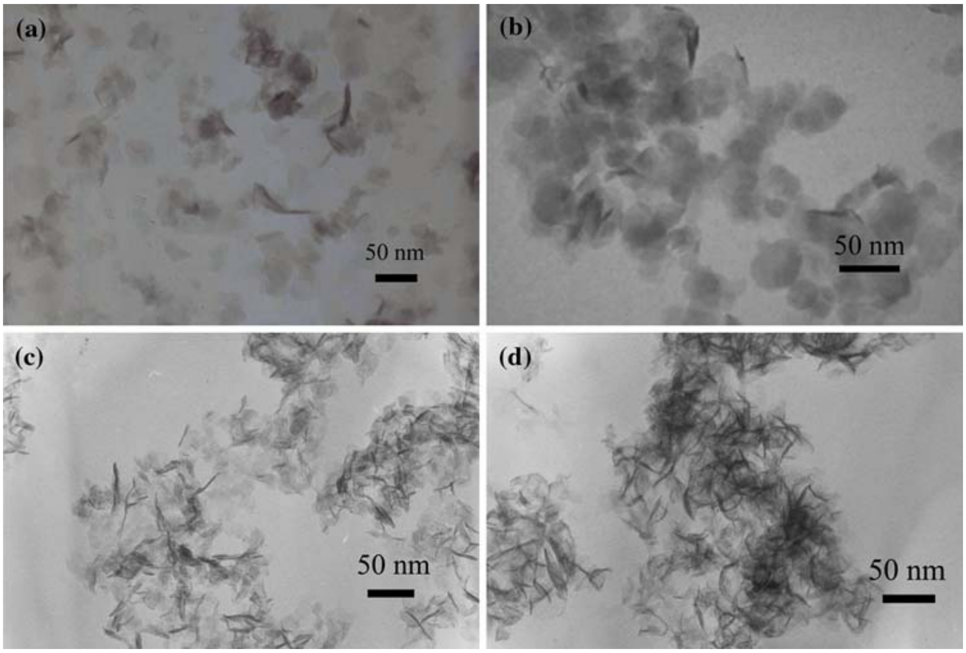

Fig. 6 TEM images for Cu_2Cr-HTlcs with different aging time for **a** 9 h; **b** 24 h; **c** 1 week; **d** 1 month

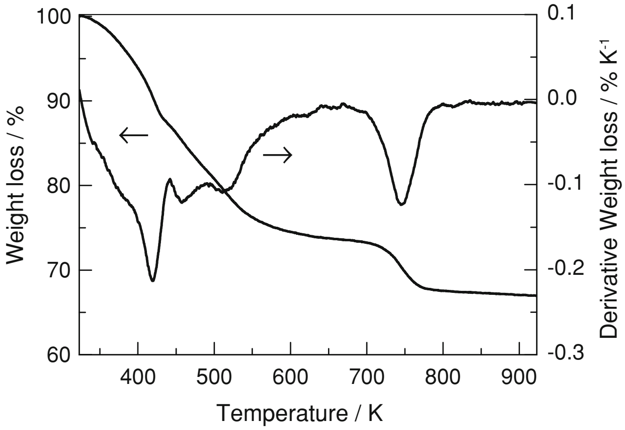

Fig. 8 TG and DTG curves for Cu/Cr-HTlcs with Cu/Cr molar ratios of 2:1 aging for 24 h

740 K is shown on the DTG curve. The total weight loss is around 33 wt%.

Generally, for Mg/Al-hydrotalcites, such a weight loss (due to decarbonation and dehydroxylation) extends up to ca. 670 K, and no further weight loss is usually recorded above this temperature [19]. However, in the case of transition metal containing hydrotalcites, particularly with those containing copper, an endothermic high-temperature effect around 873 K, was observed [20–22]. Velu and Swamy [21] have observed this effect for Cu/Mn/Al hydrotalcite and attributed this feature to a reaction occurring between brucite sheets and carbonate anions to form an oxycarbonate of chemical composition $M(II)M(III)_xO_y(CO_3)_z$ [20]. However, Alejandre et al. [22] have found a similar thermal feature in an attempt to synthesize pure Cu/Al hydrotalcites and attributed this to differences in the coordination of carbonate anions within the brucite-like lattice. It was also reported that the thermal decomposition mechanism of Mg/Al-hydrotalcites corresponded to the functional form of $(1-\alpha)^{-1} - 1$. Here our Cu/Cr-HTlcs sample decomposes at 740 K, this temperature is relatively higher than Mg/Al hydrotalcites and is lower than other Cu-containing hydrotalcites. This lower stability can be ascribed to the Jahn–Teller effect of Cu, and Cu is the only divalent cation in Cu/Cr-HTlcs which means there is no other divalent metal to weaken the Jahn–Teller effect. And the Jahn–Teller effect of Cu, which leads to a distortion of the texture, and this distortion results in a compartment of close contiguous Cr_2O_3 and an improvement of disperse for chromium. Thus the sample collapses in a different approach. This confirms the argument of TEM analysis. And the lower stability of Cu/Cr-HTlcs may make it possible for application as a good catalyst after calcination.

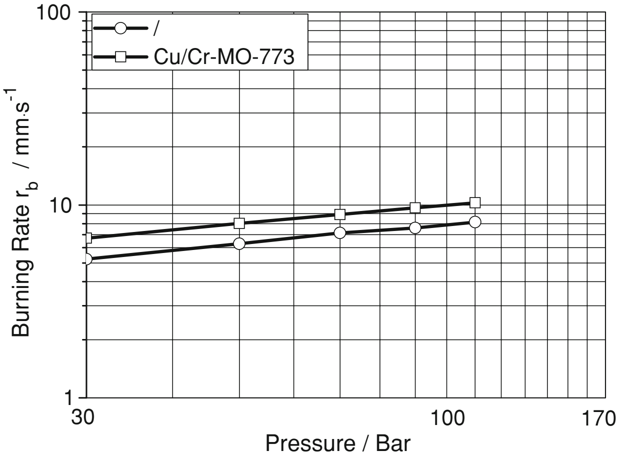

Fig. 9 Steady burning rate for solid propellants in the pressure range 30–110 bar

Catalytic performance of Cu/Cr-MO catalysts

Steady burning rate for solid rocket propellants in the pressure range 30–110 bar was measured. As shown in Fig. 9, propellant with Cu/Cr-MO-773 catalysts exhibits significantly higher burning rate than the fresh propellant over the whole explored pressure. From Table 2 we can see that the press index for catalyzed propellant almost decreases by 26.5% from 0.339 to 0.299. Experimental tests performed with Cu/Cr-MO catalysts show a large increase in steady burning rate and decrease for press index may be caused by the good dispersion and large specific surface areas of the catalyst, which improves the combustion of propellant.

Catalytic performances of different catalysts on combustion of propellant were also studied. As shown in Table 3, the propellant has a much higher burning rate of 9.27 mm s^{-1} for catalyst based on Cu_2Cr-MO-773 and 9.64 mm s^{-1} for catalyst of Cu_2Cr-MO-1073, respectively, than non-catalyzed one of 6.28 mm s^{-1}. While the propellant with $CuO \cdot Cr_2O_3$-773 catalyst has a burning rate of 9.07 mm s^{-1}, which is lower than Cu/Cr-HTlcs derived

Table 2 Steady burning rate and burning rate equation for propellants with and without catalyst

Catalyst	Burning rate (r_b/mm s^{-1})					Burning rate equation (30–110 bar)
	30 bar	50 bar	70 bar	90 bar	110 bar	
–	5.235	6.287	7.151	7.584	8.140	$r_b = 3.632\ P^{0.339}$
Cu_2Cr-MO	6.722	8.014	8.904	9.650	10.254	$r_b = 4.834\ P^{0.299}$

Table 3 Combustion properties and mechanical performance of solid propellants with different burning rate catalysts

Catalyst	T/K	σ_m/MPa	ε_b/%	ε_m/%	r_6/mm s^{-1}	Catalytic effect
–	293	0.78	69.0	59.6	6.28	–
	323	0.50	74.2	47.8		
	233	2.35	73.9	47.2		
Cu_2Cr-MO-773	293	0.66	69.1	57.5	9.27	47.61
	323	0.55	66.3	54.3		
	233	2.24	80.0	70.2		
Cu_2Cr-MO-1073	293	0.44	83.4	59.7	9.64	53.50
	323	0.36	92.4	59.2		
	233	1.65	79.8	65.2		
$CuO \cdot Cr_2O_3$-773	293	0.96	54.6	48.0	9.07	44.43
	323	0.81	50.0	43.4		
	233	2.08	51.1	42.2		

catalysts. And the burning rate of propellant at 60 bar with catalyst dosage of 1.0 wt% is higher than the one of 0.5 wt% (ca. 8.46 mm s^{-1}, calculated from Fig. 9), which means that burning rate increases with the dosage of catalysts. The mechanical performance of break elongation (ε_b) and maximum elongation (ε_m) at different temperature for propellants with Cu/Cr hydrotalcite derived catalysts as exhibited in Table 3 are enhanced or comparative to the non-catalyzed ones, while $CuO \cdot Cr_2O_3$ catalyzed one has rather lower values. By contrary, maximum tensile strength (σ_m) of Cu/Cr-MO catalyzed propellants is a bit lower than $CuO \cdot Cr_2O_3$ catalyzed one. Our study indicates that the Cu/Cr hydrotalcite derived catalysts can enhance elongation properties of the propellants, while the $CuO \cdot Cr_2O_3$ catalysts, are obtained by mechanically mixing the CuO and Cr_2O_3, has a clear improvement for tensile strength of propellants.

In summary, experimental tests performed with Cu/Cr-HTlcs derived mixed oxides catalyzed propellants show a large increase in the steady burning rate and decrease in press index, and mechanical performance on elongation has a clear enhancement.

Conclusions

In conclusion, pure and well-crystallized Cu/Cr-HTlcs with Cu/Cr molar ratio of 2:1 was successfully prepared by coprecipitation reaction. No other companion phases were seen in the sample ascribed to the lower Cu^{2+} ions concentration and content, which weakened the Jahn–Teller effect of copper. And Cu/Cr-HTlcs exhibit homogenous hexagons morphology with average crystallite size in the range of 30–50 nm when aging time reached 24 h, while the flakes tend to curl if kept for prolonged aging time. The material has a specific surface area of 107.8 m^2 g^{-1} and an average pore diameter of 9 nm with pore volume of 0.34 cm^3 g^{-1}. N_2 adsorption–desorption isotherm graphic of Cu/Cr-HTlcs is type IVb with H_2-type hysteresis loop, and it can be easily transformed into mixed oxides under lower temperature at about 740 K, which makes it attractive for catalytic applications. Solid propellant with Cu/Cr-MO-1073 catalyst exhibits higher burning rate of 9.64 mm s^{-1} than those with $CuO \cdot Cr_2O_3$ catalys/without catalyst, and press index decreases by 26.5%. Mechanical performance for Cu/Cr-MO catalyzed propellant has a clear improvement on elongation.

Acknowledgement Financial supports from the Final Assembly Line "15" pre-research (No. 41328030507) fund are gratefully acknowledged.

References

1. Cavani F, Trifiro F, Vaccari A (1991) Catal Today 11:173
2. Shen JY, Guang B, Tu M (1996) Catal Today 30:77
3. Centi G, Perathoner S (2007) Appl Catal B Environ 70:172
4. Palomares AE, Uzcàtegui A, Corma A (2008) Catal Today 137:261
5. Trujillano R, Holgado MJ, González JL (2005) Solid State Sci 7:931
6. Shiau CY, Chen S, Tsai JC, Lin SI (2000) Appl Catal A Gen 198:95
7. Mónica C, Celso P, Julio F, Griselda E, Eduardo H, Sandra C, Enrique RC (2007) Appl Catal A Gen 317:11
8. Iglesias AH, Ferreira OP, Gouveia DX (2005) Solid State Chem 178:142
9. Meda L, Marra G, Galfetti L, Inchingalo S, Severini F, De Luca L (2005) Compos Sci Technol 65:769
10. Wang BY, Feng ZG, Yang RJ (1997) Powder burning theory. Beijing Institute of Technology Press, Beijing
11. Dokhan A, Price EW, Seitzman JM, Sigman RK (2002) Proc Combust Inst 29:2939
12. Galfetti L, DeLuca LT, Severini F, Colombo G, Meda L, Marra G (2007) Aerosp Sci Technol 11:26
13. Liu LL, Li FS, Tan LH (2007) J Solid Rocket Technol 30:52
14. Chen AS, Li FS, Ma ZY, Liu HY (2004) J Solid Rocket Technol 27:123
15. Chai YP, Zhang TL (2007) J Solid Rocket Technol 30:44
16. Cudennec Y, Lecerf A (2003) Solid State Sci 5:1471
17. Trifiro F, Vaccari A (1996) In: Atwood JL (ed) Comprehensive supramolecular chemistry. Pergamon Press, Oxford
18. Rouquerol F, Rouquerol J, Sing KSW (1999) Adsorption by powders and porous solids. Principles, methodology and applications. Academic Press, London
19. Kannan S, Velu S, Ramkumar V, Swamy CS (1995) J Mater Sci 30:1462. doi:10.1007/BF00375249
20. Kannan S, Rives V, Knözinger H (2004) Solid State Chem 177:319
21. Velu S, Swamy CS (1996) J Mater Sci Lett 15:1674
22. Alejandre A, Medina F, Salagre P, Corregi X, Sueiras JE (1999) Chem Mater 11:939